

Sudan University of Science and Technology

College of Graduate Studies



**Evaluation of Liver Tumors by Using Triphasic Spiral Computed
Tomography**

تقويم أورام الكبد باستخدام الأشعة المقطعية ثلاثة الطور

A Thesis Submitted in Partial Fulfillment for M.Sc. Degree in Diagnostic
Radiological Technology

By: Jihad Hamid Gad Elmoula Mohamed

Supervisor: Dr. Babikir Abd Alwahab Awad Allah

February 1, 2016

بسم الله الرحمن الرحيم

قُلْ يِعْبَادِيَ الَّذِينَ أَسْرَفُوا عَلَىٰ أَنْفُسِهِمْ لَا تَقْنَطُوا مِنْ رَحْمَةِ اللَّهِ ۖ
إِنَّ اللَّهَ يَغْفِرُ الذُّنُوبَ جَمِيعًا ۖ إِنَّهُ هُوَ الْغَفُورُ الرَّحِيمُ (٥٣)

سورة الزمر الآية 53

صدق الله العظيم

Dedication

I thank my parents for the unconditional support with my study, I'm honored to have you as my parents. Thank you for giving me a chance to prove and improve myself through all my walk of life.

I thank my family for believing in me.

My brothers hoping that with this research I have proven to you that there is no mountain can stop your ambition and dreams.

Acknowledgment

Thanks to Dr. Babiker Abd Elwahab Awad Alla, my supervisor for his close supporting me to complete this research.

I would like also to thank Dr.Mohamed Ali for his help in collecting data.

My thanks to Dr.Ahmed Mohammed Mahmoud, who helped me too much.

Special thanks to my best friends Dr. Abd Elsalam Abas & Dr.Namariq Ahmed & Dr. Mohamed Jamal who help me in this study from the beginning.

Abstract

This is a retrospective and practical study which was done during August-2015 to February 2016 and was carried out in Police University Hospital and Royal Scan International Hospital. Khartoum - Sudan.

The study discusses evaluation of liver tumors using triphasic spiral CT.

A total of “50” patients were selected randomly; male (24) and female (26) all those patients have age above 35 years, have signs of liver disorders and referred by physician.

All patients were subjected to be examined by CT scanners using Toshiba CT scanner 64 slice and Neo Soft 16 slice, laboratory (RFT, Creatinine).

Ct abdominal scan performed for all patients after injection of contrast media intravenously.

The study used the time of contrast media to reach the tumor, the time of leaving and the type of enhancement to differentiate between benign and malignant tumors.

The results shown that the common liver tumors are malignant (72%) appears as hyper-dense area related to liver parenchyma at arterial phase due to it hyper vascularity and reaching of contrast rapidly (rapid wash-in), and hypo-dense area at venous phase due to rapid wash-out, and most frequently seen at the age between 54-62 years old (32%) with metastases at different organs (Kidney-Pancreas-Gall Bladder and Urinary Bladder) and most common in females than males, and benign tumors (28%) appear as peripheral hyper-dense area related to liver parenchyma at arterial phase due to it hypo-vascularity and

reach of contrast slowly, or non-vascular (enhancement), and hyper-dense area at venous phase due to low wash-out of contrast from tumor.

Study concludes that Tri-phasic spiral CT is the golden standard modality to evaluate the liver tumors and give clearly image of normal liver parenchyma and any pathology that affect it.

المستخلص

هذه الدراسة وصفية وعملية أجريت خلال الفترة من أغسطس 2015م إلي فبراير 2016م وطبقت في مستشفى الشرطة الجامعي ومستشفى رويال سكان العالمية. ولاية الخرطوم بجمهورية السودان.

الدراسة ناقشت دور الأشعة المقطعية ثلاثية الطور في تقييم أورام الكبد الحميدة والخبيثة.

هنالك (50) مريض أختيروا عشوائياً، (24) ذكر و (26) أنثى، أعمارهم فوق 35 سنة ولديهم أعراض أمراض الكبد ومرسلين بواسطة الطبيب.

جميع المرضى أجري لهم فحص الأشعة المقطعية بأجهزة توشيا (64 شريحة) و نيو سوفت (16 شريحة) وفحوصات معملية (فحص وظائف الكلي، كريتانين).

أجري فحص الأشعة المقطعية للبطن مع حقن صبغة ملونة وريديا وذلك للتمييز بين الأورام الخبيثة والحميدة باستخدام زمن دخول الصبغة وزمن خروجها من الورم وشكل التباين داخل الورم.

أظهرت النتائج أن الأورام الأكثر إنتشاراً هي الخبيثة بنسبة (72%) وتظهر منطقة ذو قيمة لونية عالية في الحالة الشريانية مقارنة بأنسجه الكبد، نسباً لأنها تحتوي علي تغذية دموية عالية، وذلك يسهل وصول الصبغة بسرعة للورم، ومنطقة ذو قيمة لونية أقل في الحالة الوريدية وذلك لخروج الصبغة من الورم بصورة سريعة، وأكثر الفئات عرضة للإصابة هم الإناث في العمر ما بين 54-62 سنة، مع وجود إنتشار للخلايا السرطانية في أعضاء أخرى (الكلي-المثانة-الحويصلة الصفراوية-البنكرياس). أما الأورام الحميدة بنسبة (28%) وتظهر ذو قيمة لونية أعلى بقليل من أنسجه الكبد في الحالة الشريانية، وذلك لتخلل الصبغة بصورة بطيئة داخل الورم، وذو قيمة لونية عالية في الحالة الوريدية وذلك لبطئ خروج الصبغة من داخل الورم.

الدراسة وجدت أن للأشعة المقطعية ثلاثية الطور دور كبير في التمييز بين أمراض الكبد الحميدة والخبيثة، وتوضيح وجود أي شوائب داخل أنسجه الكبد السليمة.

LIST OF TABLES

Table no	Subject	Page
2-1	Comparison of the parameters of different scan modes AFOV – axial field of view, p – pitch.	25
2-2	Parameters are usually selectable on a cone-beam CT system console	26
2-3	Show different HU for different densities	37
4-1	Distribution of population by gender	44
4-2	Shows distribution of liver tumors by gender	44
4-3	Shows distribution of liver tumors by age	45
4-4	Show degree of enhancement of tumor related to liver parenchyma	46

LIST OF FIGURES

Figure no	Subject	Page
2-1	The morphological lobes of the liver	3
2-2	Distribution of hepatic arteries	7
2-3	Hepatobiliary system	10
2-4	CT crossectional abdominal image	11
2-5	Raw data processing and reconstruction steps in a cone-beam CT system	28
2-6	Offset image of a 7-panel detector without correction	29
2-7	Image of a 7-panel detector without gain correction	30
2-8	The X-ray detector illumination response function	30
2-9	Beam-hardening effect and correction	32
3-1	Automatic injector	42
3-2	CT Scanner and control console	42
4-1	Distribution of population by gender	44
4-2	Shows distribution of liver tumors by gender	45
4-3	Shows distribution of liver tumors by age	46
4-4	Shows correlation between degree of enhancement of benign and malignant tumor with time	47
A-1	Axial CT image:large liver mass (HCC) with central necrosis	51

A-2	Coronal CT image:large liver mass (HCC) with central necrosis	51
A-3	Axial Tri-phasic CT images with and without contrast showed two calcified tumors	52
A-4	Axial tri-phasic spiral CT images shown HCC with metastases in left kidney	52

LIST OF CONTENTS

Content	Page
الآية	i
Dedication	ii
Acknowledgment	iii
English abstract	iv
ملخص البحث	vi
List of tables	vii
List of figures	viii
List of content	x
List of abbreviation	xiv
Chapter one	
1-1 Introduction	1
1-2 problem of the study	2
1-3 Objectives of the study	2
1-3-1 General objectives	2
1-3-2 Specific objectives	2
1-4 Overview of the study	2
Chapter two (Literature review)	
2-1 Liver	3
2-1-1 Anatomy	3
2-1-2 Structure	4
2-1-3 Segmental anatomy	4
2-1-4 Peritoneal attachments	6

2 -1-5Portal Hepatic System	7
2-1-6 Vasculature	7
2-2 GB and hepatobiliary system	10
2-3 Physiology	14
2-3-1 Regulations	14
2-3-2 Glucose	14
2-3-3 Proteins	14
2-3-4 Bile	14
2-3-5 Lipids	15
2-3-6 Storage	15
2-3-7 Purification, transformation and clearance	15
2-3-8 Ammonia	16
2-3-9 Bilirubin	16
2-3-10 Hormones	16
2-3-11 Drugs	16
2-3-12 Toxins	17
2-4 Regeneration of the Liver	17
2-4-1 The Dynamics of Liver Regeneration	18
2-4-2 Stimuli of Hepatic Regeneration	19
2-5 Pathology	19
2-5-1 Cirrhosis	19
2-5-2 Glycogen storage disease	20
2-5-3 Fatty liver	20
2-5-4 Cyst	20
2-5-5 Abscess	20
2-5-6 Tumors	20

2-5-6-1 Benign	20
2-5-6-2 Malignant	22
2-5-7 Metastases	23
2.6 Computed tomography	23
2-6-1 Introduction	23
2-6-2 Basic principles	24
2-6-3 Data acquisition	25
2-6-3-1 Data acquisition modes	25
2-6-3-2 Circular scan	26
2-6-3-3 Spiral scan	26
2-6-3-4 Other orbits	27
2-6-3-5 Acquisition parameters	28
2-6-3-6 Raw data processing	29
2-6-4 Corrections	30
2-6-4-1 Offset correction	30
2-6-4-2 Gain correction	31
2-6-4-3 Beam-hardening correction	33
2-6-4-4 Bad pixel correction	34
2-6-4-5 Geometric calibration	35
2-6-5 Image display	36
2-6-5.1 CT number	37
2-6-6 Instruments	38
2-6-7 Advantage & disadvantage	38
2-6-7-1 Advantage	38
2-6-7-2 Disadvantage	38
2-6-8 Previous studies	39

Chapter three (Martials and methods)	
3-1 CT system	42
3-2 Population	42
3-3 Sample size	42
3-4 Patient preparation	42
3-5 Equipment	42
3-6 Contrast media	43
3-6-1 IV HO�M or LOCM	43
3-6-1-1 Total amount of contrast	43
3-6-1-2 Injection rate	43
3-6-2 Oral Contrast	43
3-7 Technique	43
3-8 Phases	43
3-8-1 Arterial	43
3-8-2 Portovenous	43
3-8-1 Venous	43
3-8-2 Delay	43
Chapter four (Results)	
Chapter five	
Discussion	48
Conclusion	49
Recommendation	49
Appendices	51
References	54

Abbreviation

aFOV	Axial field of view
CAT	Computed axial tomography
CBD	Common bile duct
CHD	Common hepatic duct
CT	Computed tomography
DNA	Deoxyribonucleic acid
FBP	Filtered back projection
FLD	Fatty liver disease
GI	Gastro intestinal
HCC	Hepato cellular carcinoma
HOCM	High-osmolar contrast media
HU	Hounsfield unit
IgA	Immune globulin A
IV	Intra venous
IVC	Inferior vena cava
LOCM	Low-osmolar contrast media
STP	Standard pressure and temperature

Chapter one

1.1 Introduction:

Spiral CT is most commonly used modality for detection and characterization of focal hepatic defects in patients with chronic liver disease. Tumor conspicuity has to be maximized to ensure its detection. For this purpose, CT is done in different phases of contrast enhancement i.e., early and late arterial and portal venous phases, it is seen that hyper vascular tumors are best seen in late arterial phase (**JRMC 2011**).

In more recent studies it is seen that most of tumors have maximum conspicuity in late arterial phase but a combination of early and late arterial phases maximizes number of tumors detected (**JRMC 2011**).

Using two arterial phases instead of one is beneficial for tumor detection. However, it exposes patients to more radiation, requires additional films, additional data storage capacity and requires more time of radiologists for reporting. Presently triphasic CT scan of liver is imaging modality of choice for detection and characterization of focal lesions of liver, for exclusion of multifocal disease, to select candidates for curative surgery, embolotherapy, radiofrequency ablation and trans-arterial chemoembolization. Helical CT scanners allow images of the entire liver to be obtained during the phase of maximum parenchymal enhancement, enabling optimal detection of focal hepatic lesions, as most of the hepatic neoplasms are relatively hypovascular (**JRMC 2011**).

Accurate detection of small hepatic neoplasms is critical to the examination of patients as they are possible candidates for curative surgery. On the other hand, some patients are referred for CT in an attempt to localize focal lesion already detected by ultrasound. CT technique used for examination of these patients should

be optimized not only for detection but also for differentiation of benign and malignant tumors (**JRMC 2011**).

In triple phase helical CT images obtained, during the phase of preferential early and late arterial enhancement can be obtained together with portovenous phase images during a single bolus injection. Different studies have shown that this technique allows improved detection of hypervascular neoplasms (**JRMC 2011**).

1.2 Problem:

Most of hospitals using venous phase instead of portovenous phase in tri-phase study, and that may lead to miss some tumors to be detected.

1.3 Objectives:

1.3.1 General objective:

The main objective of this study to evaluate liver tumors using tri-phasic spiral CT.

1.3.2 Specific objective:

To identify the type of tumor, asses the enhancement characteristic in tri-phasic CT scan performance in patients with suspected liver tumor.

1.4 Overview of the study:

This study consists of five chapters, chapter one contains introduction, problem, objectives and overview of the study. Chapter two deals with literature review which includes anatomy, physiology and pathology of the liver, CT physics and previous studies. Chapter three contains methodology of the study. Chapter four contains results of the study. Chapter five contains discussion of the results, conclusion and recommendations. Finally, there are lists of references, appendices which include CT images and data collection sheet.

Chapter two

2.1 Liver:

2.1.1 Anatomy:

This is the largest organ in the body, it is related by its domed upper surface to the diaphragm, which separates it from pleura, lungs, pericardium and heart. Its posteroinferior (or visceral) surface abuts against the abdominal esophagus, the stomach, duodenum; hepatic flexure of colon and the right kidney and suprarenal, as well as carrying the gall-bladder (**Harold Ellis 2006**).

The liver is divided into a larger right and small left lobe, separated superiorly by the falciform ligament and posteroinferiorly by an H-shaped arrangement of fossae Figure (2.1) (**Harold Ellis 2006**).

The biliary system is composed of the gallbladder and bile ducts (both intrahepatic and extrahepatic) that serve to drain the liver of bile and then store it until it is transported to the duodenum to aid in digestion. The hollow pear-shaped gallbladder is located in the gallbladder fossa on the anteroinferior portion of the right lobe of the liver, closely associated with the main lobar fissure. It functions as the reservoir for storing and concentrating bile before being transported to the duodenum. The gallbladder can be divided into a fundus, body, and neck the fundus is the rounded distal portion of the gallbladder sac that is frequently in contact with the anterior abdominal wall. The widest portion, the body, gently tapers superiorly into the neck, the narrow neck lies to the right of the portohepatis and continues as the cystic duct. The neck contains circular muscles that create spiral folds within the mucosa that are called the spiral valves of Heister, these valves are especially prominent at the bend formed by the neck and cystic duct, a common area for gallbladder impaction during acute or chronic cholecystitis. The gallbladder has a muscular wall that contracts when stimulated by cholecystokinin,

forcing bile through the extrahepatic biliary system into the duodenum (**Harold Ellis 2006**).

2.1.2 Structure:

The liver is made up of lobules, each with a solitary central vein which is a tributary of the hepatic vein which in turn, drains into the inferior vena cava.

In spaces between the lobules, termed portal canals, lie branches of the hepatic artery (bringing systemic blood) and the portal vein, both of which drain into the central vein (**Harold Ellis 2006**).

2.1.3 Segmental anatomy:

The gross anatomical division of the liver into a right and left lobe, demarcated by a line passing from the attachment of the falciform ligament on the anterior surface to the fissures for the ligamentum teres and ligamentum venosum on its posterior surface, is simply a gross anatomical descriptive term with no morphological significance (**Harold Ellis 2006**).

Studies of the distribution of the hepatic blood vessels and ducts have indicated that the true morphological and physiological division of the liver is into right and left lobes demarcated by a plane which passes through the fossa of the gall-bladder and the fossa of the inferior vena cava. Although these two lobes are not differentiated by any visible line on the dome of the liver, each has its own arterial and portal venous blood supply and separate biliary drainage. This morphological division lies to the right of the gross anatomical plane and in this the quadrate lobe comes to be part of the left morphological lobe of the liver while the caudate lobe divides partly to the left and partly to the right lobe, the right and left morphological lobes of the liver can be further subdivided into a number of segments, four for each lobe (**Figure 2.1**) (**Harold Ellis 2006**).

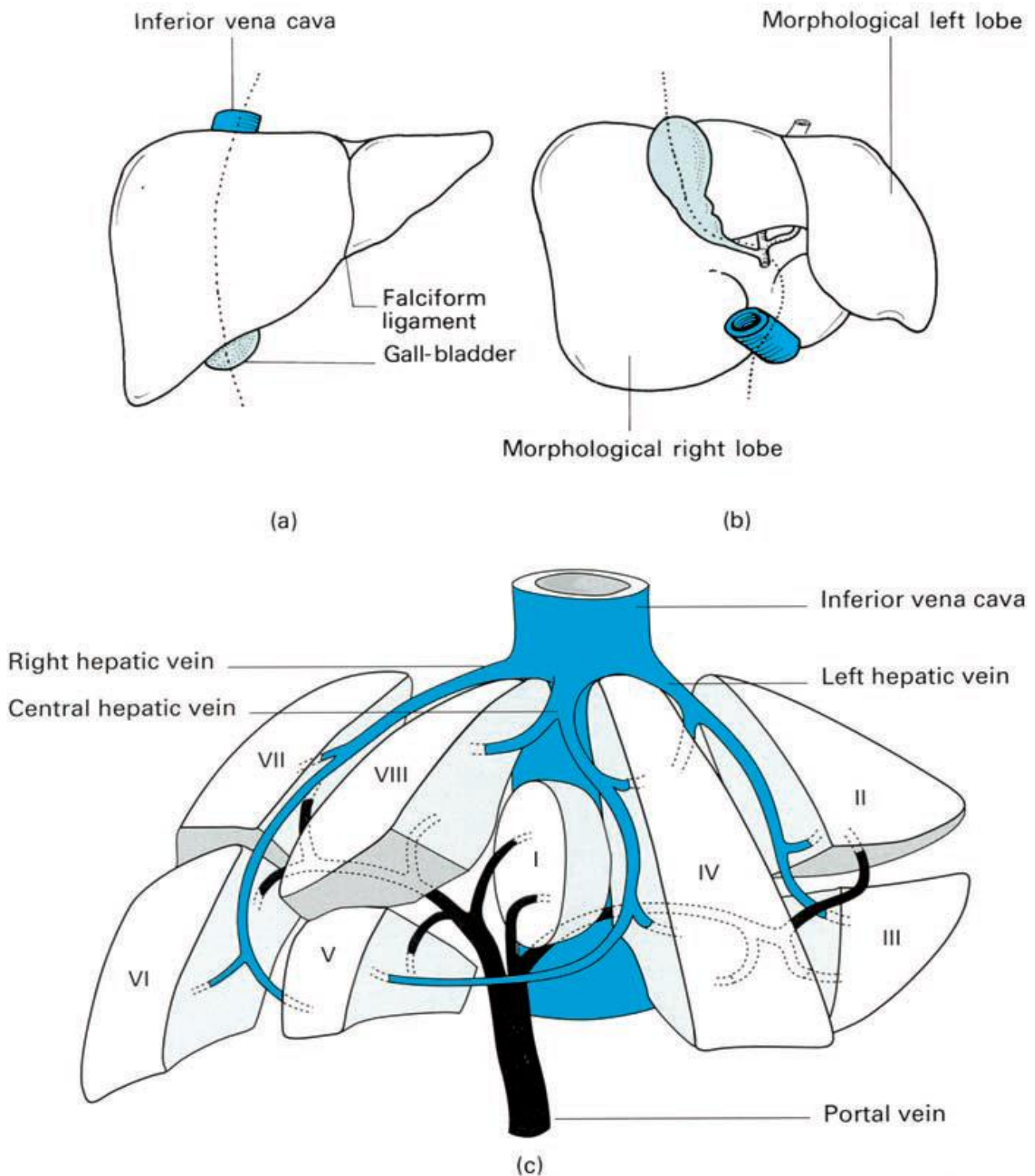


Figure (2.1): The morphological right and left lobes of the liver shown separated by the dotted line: (a) anterior and (b) ventral aspect. Note that the quadrate lobe is morphologically a part of the left lobe while the caudate lobe belongs to both right and left lobes. (c) The further segmental divisions of the liver (**Harold Ellis 2006**).

The student need not learn the details of these, but of course to the hepatic surgeon, carrying out a partial resection of the liver, knowledge of these segments, with their individual blood supply and biliary drainage, is of great importance. at the hilum of the liver, the hepatic artery, portal vein and bile duct each divide into right and left branches and there is little or no anastomosis between the divisions on the two sides (**Harold Ellis 2006**).

From the region of the porta hepatis, the branches pass laterally and spread upwards and downwards throughout the liver substance, defining the morphological left and right lobes (**Harold Ellis 2006**).

2.1.4 Peritoneal attachments:

The liver is enclosed in peritoneum except for a small posterior bare area, demarcated by the peritoneum from the diaphragm reflected on to it as the upper and lower layers of the coronary ligament. To the right, these fuse to form the right triangular ligament (**Harold Ellis 2006**).

The falciform ligament ascends to the liver from the umbilicus, somewhat to the right of the midline, and bears the ligamentum teres in its free border.

The ligamentum teres passes into its fissure in the inferior surface of the liver while the falciform ligament passes over the dome of the liver and then divaricates. Its right limb joins the upper layer of the coronary ligament and its left limb stretches out as the long narrow left triangular ligament which, when traced posteriorly and to the right, joins the lesser omentum in the upper end of the fissure for the ligamentum venosum (**Harold Ellis 2006**).

The lesser omentum arises from the fissures of the porta hepatis and the ligamentum venosum and passes as a sheet to be attached along the lesser curvature of the stomach (**Harold Ellis 2006**).

2.1.5 Portal Hepatic System:

The liver receives nutrient-rich blood from the gastrointestinal tract via the portal hepatic system (**Hiatt 1994**).

The major vessel of this system is the portal vein, which is formed in the retroperitoneum by the union of the superior mesenteric and splenic veins, posterior to the neck of the pancreas. It passes obliquely to the right, posterior to the hepatic artery within the lesser omentum, and enters the liver at the porta hepatis. At the porta hepatis, the portal vein branches into right and left main portal veins that then follow the course of the right and left hepatic arteries.

The right portal vein first sends branches to the caudate lobe, then divides into anterior and posterior branches that subdivide into superior and inferior branches to supply the right lobe of the liver. Left portal vein initially courses to the left, then turns medially toward the ligamentum teres (**Hiatt 1994**).

It branches to supply the lateral segments (segments II and III) of the left lobe and the superior and inferior segmental branches of segment IV (**Hiatt 1994**).

2.1.6 Vasculature:

The liver is unusual in that it has a dual blood supply, receiving arterial blood (20%-25%) from the common hepatic artery and nutrient-rich venous blood (75%-80%) from the portal vein (**Hiatt 1994**).

The common hepatic artery usually arises as one of the three branches off the celiac artery, coursing to the right to enter the lesser omentum anterior to the portal vein. It branches into the right gastric and gastroduodenal arteries just above the duodenum and continues in the hepatoduodenal ligament as the proper hepatic artery (**Hiatt 1994**).

While within or just before entering the porta hepatis, the proper hepatic artery divides into left and right hepatic arteries that continue to branch and supply the lobes of the liver (**Hiatt 1994**).

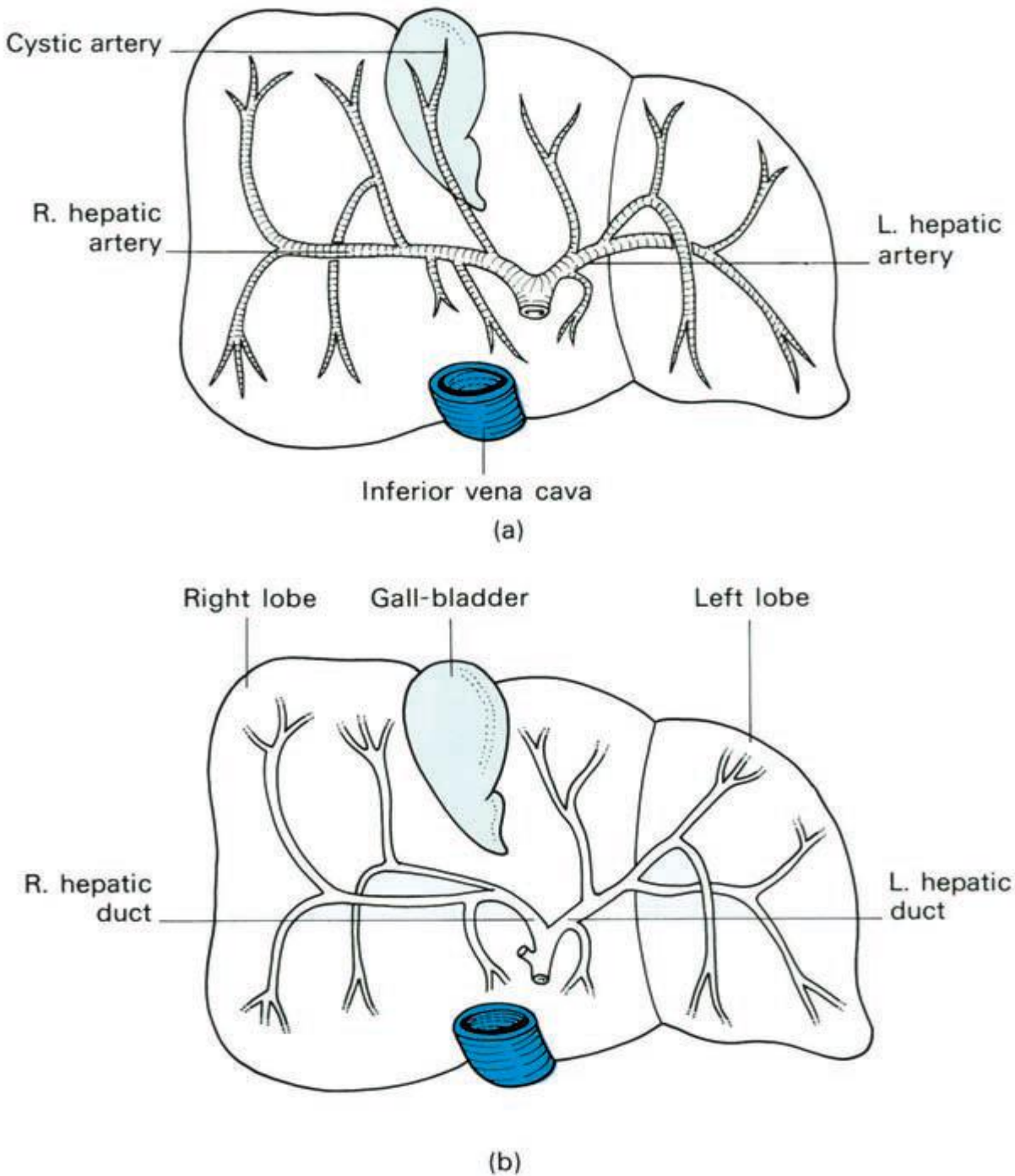


Figure (2.2): (a) Distribution of hepatic arteries. (b) Distribution of hepatic biliary ducts.

Note that the quadrate lobe is supplied exclusively by the left hepatic artery and drained by the left hepatic duct. The caudate lobe is supplied by each (Hiatt 1994).

The right hepatic artery is larger than the left and supplies the majority of the right lobe of the liver. It passes posterior to the uncinate process of the pancreas and runs along the posterior wall of the bile duct into the right hepatic lobe. The left hepatic artery is located between the lesser curvature of the stomach and approaches the liver in the lesser omentum and branches to supply the caudate, quadrate, and medial and lateral segments of the left lobe of the liver. The venous drainage of the liver occurs via the small interlobar and intersegmental hepatic vessels that merge into the three major hepatic veins, emptying directly into the IV, just below the diaphragm. The right hepatic vein, the largest, lies between the right anterior and posterior hepatic segments, drains segments V, VI, and VII, and enters the IV at the right lateral aspect. The middle hepatic vein lies in the interlobar fissure, drains segments IV, V, and VIII, then enters the IV at the anterior or right anterior surface. The smallest hepatic vein, the left hepatic vein, courses between the medial and lateral segments of the left lobe, drains segments II and III, then enters the left anterior surface of the IV (**Hiatt 1994**).

Frequently, the middle and left hepatic veins converge to form a common trunk before emptying into the IV just below the diaphragm. The IV lies in a groove along the posterior wall of the liver and ascends into the thoracic cavity through the caval hiatus of the diaphragm and enters the right atrium of the heart (**Hiatt 1994**).

2.2 GB and hepatobiliary system:

The biliary system is composed of the gallbladder and bile ducts (both intrahepatic and extrahepatic) that serve to drain the liver of bile and then store it until it is transported to the duodenum to aid in digestion. The hollow pear-shaped gallbladder is located in the gallbladder fossa on the anteroinferior portion of the right lobe of the liver, closely associated with the main lobar fissure. It functions as

the reservoir for storing and concentrating bile before being transported to the duodenum. The gallbladder can be divided into a fundus, body, and neck, the fundus is the rounded distal portion of the gallbladder sac that is frequently in contact with the anterior abdominal wall. The widest portion, the body, gently tapers superiorly into the neck. The narrow neck lies to the right of the porta hepatis and continues as the cystic duct. The neck contains circular muscles that create spiral folds within the mucosa that are called the spiral valves of Heister. These valves are especially prominent at the bend formed by the neck and cystic duct, a common area for gallbladder impaction during acute or chronic cholecystitis. The gallbladder has a muscular wall that contracts when stimulated by cholecystokinin, forcing bile through the extrahepatic biliary system into the duodenum. Bile, formed within the liver, is collected for transport to the gallbladder by the intrahepatic bile ducts. The intrahepatic bile ducts run beside the hepatic arteries and portal veins throughout the liver parenchyma. The intrahepatic duct merge into successively larger ducts as they follow a course from the periphery to the central portion of the liver, eventually forming the right and left hepatic ducts **(Hiatt 1994)**.

The right and left hepatic ducts unite at the porta hepatis to form the proximal portion of the common hepatic duct (CHD), which marks the beginning of the extrahepatic biliary system **(Hiatt 1994)**.

The CHD is located anterior to the portal vein and lateral to the hepatic artery in its caudal descent from the porta hepatis. As the CHD descends in the free border of the lesser omentum, it is joined from the right by the cystic duct to form the common bile duct (CBD). The CBD continues a caudal descent along with the hepatic artery and portal vein within the hepatoduodenal ligament. It curves slightly to the right, away from the portal vein, then courses posterior and medial to the first part of the duodenum behind the head of the pancreas **(Hiatt 1994)**.

The CBD follows a groove on the posterior surface of the pancreatic head, then pierces the medial wall of the second part of the duodenum along with the main pancreatic duct (duct of Wirsung) through the ampulla of Vater. The ends of both ducts are surrounded by the circular muscle fibers of the sphincter of Oddi (**Hiatt 1994**).

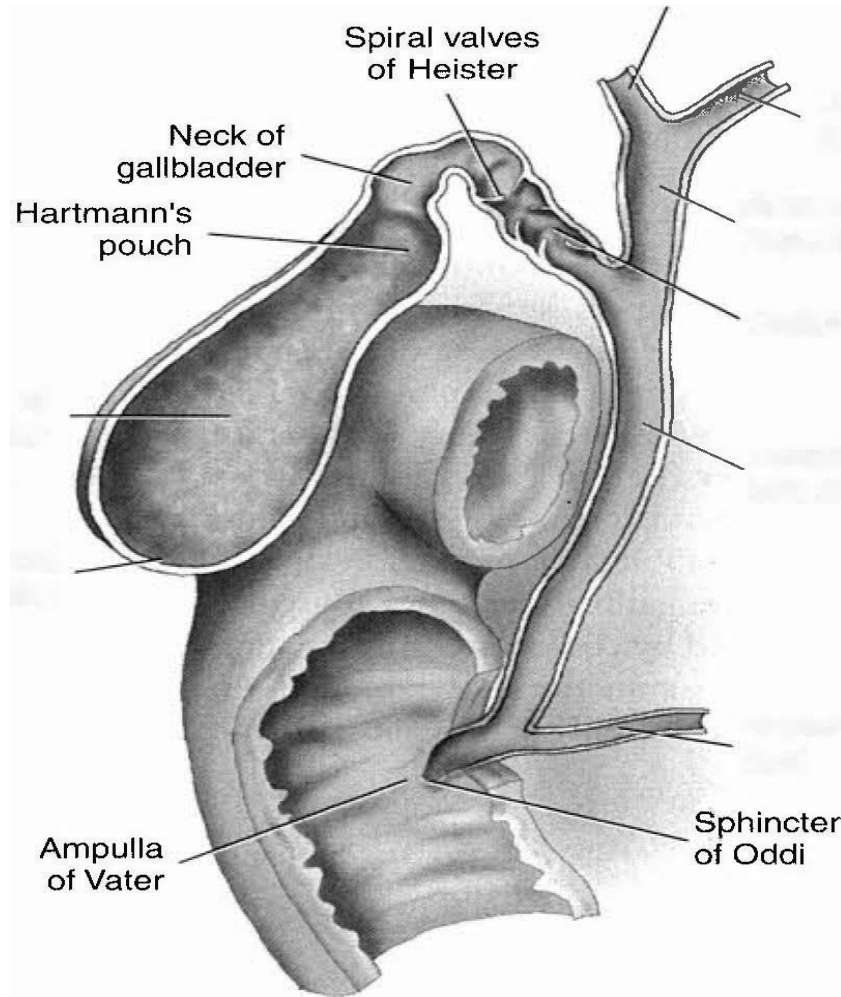


Figure (2.3) Hepatobiliary system (Hiatt 1994).

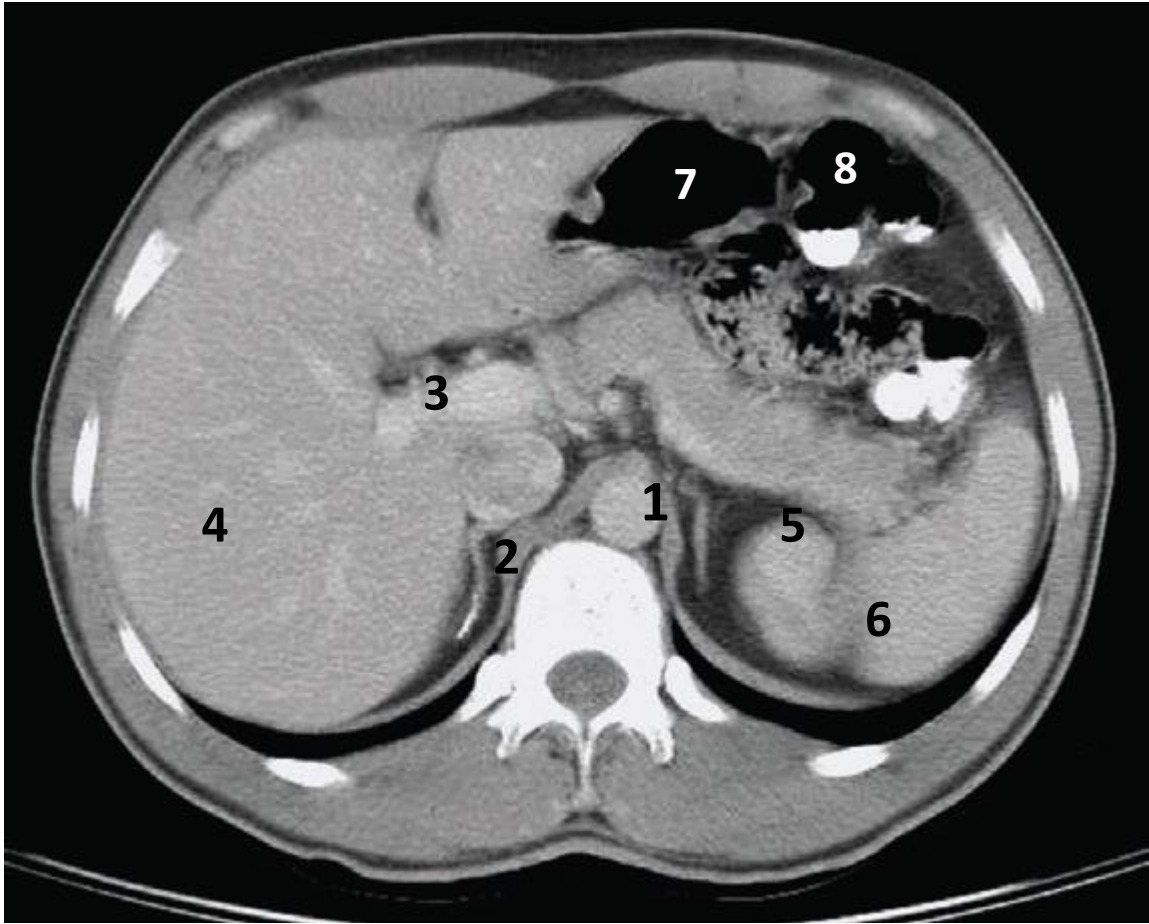


Figure (2.4): CT crossectional abdominal image (Iannaccone R et.al 2007).

- | | |
|----------------|-----------|
| 1.Aorta | 2. IVC |
| 3.Portals vein | 4. Liver |
| 5. Pancreas | 6. spleen |
| 7.Stomach | 8. colon |

2.3 Physiology:

2.3.1 Regulations:

Hepatocytes are metabolically active cells they are involved in regulation of various biochemical and metabolic functions and are involved in synthesis of various substances in the body. They take up glucose, minerals, and vitamins from portal and systemic blood and store them. Many important substances such as blood clotting factors, transporter proteins, cholesterol, and bile components are synthesized by the hepatocytes. The hepatocytes also regulate blood levels of substances such as cholesterol and glucose, the liver helps maintain body homeostasis (<http://nlfindia.com/liverzone/functions.asp>).

2.3.2 Glucose:

The liver store glucose when it is in excess after the person has food and release glucose in the blood when he is starving. This is an important function which when impaired during liver disease, result in hypoglycemia (low blood glucose) (<http://nlfindia.com/liverzone/functions.asp>).

2.3.3Proteins:

Most blood proteins (except for antibodies) are synthesized and secreted by the liver. One of the most abundant serum proteins is albumin. Impaired liver function results in decreased serum albumin level. The liver also produces most of the proteins responsible for blood clotting, called coagulation or clotting factors. Hence in severe liver disease, excessive bleeding may result due to lack of these factors (<http://nlfindia.com/liverzone/functions.asp>).

2.3.4 Bile:

Hepatocyte synthesize bile. Bile is a greenish fluid containing cholesterol, phospholipids, bilirubin (a metabolite of red blood cell hemoglobin), and bile salts.

It is secreted into biliary ducts. It then leaves the liver to be temporarily stored in the gallbladder before emptying into the small intestine. Bile salts act as "detergents" that aid in the digestion and absorption of dietary fats. Liver damage or obstruction of a bile duct (e.g., gallstone) can lead to cholestasis, (the blockage of bile flow, which causes the malabsorption of dietary fats), steatorrhea (foul-smelling diarrhea caused by non-absorbed fats), and jaundice (<http://nlfindia.com/liverzone/functions.asp>).

2.3.5 Lipids:

Liver synthesizes cholesterol. It is then packaged and distributed to the body or excreted into bile for removal from the body. Increased cholesterol concentrations in bile may predispose to gallstone formation. The liver also synthesizes lipoproteins. These are made up of cholesterol, triglycerides phospholipids, and proteins. Lipoproteins transfers cholesterol between the liver and body tissues. Most liver diseases do not significantly affect serum lipid levels. However, cholestatic diseases, may be associated with increased levels (nlfindia.com/liverzone/functions.asp).

2.3.6 Storage:

As mentioned above, the liver store important substances e.g. glucose (in the form of glycogen). The fat-soluble vitamins (vitamins A, D, E and K), folate, vitamin B 12, and minerals such as copper and iron (nlfindia.com/liverzone/functions.asp).

2.3.7 Purification, transformation and clearance:

The liver removes harmful substances (such as ammonia, toxins, various drugs) from the blood and then breaks them down or transforms them into less harmful compounds (nlfindia.com/liverzone/functions.asp).

2.3.8 Ammonia:

The liver converts ammonia to urea. Urea is then excreted into the urine by the kidneys. In the presence of severe liver disease, ammonia accumulates in the blood because of both decreased blood clearance and decreased ability to form urea. Elevated ammonia levels can be toxic, especially to the brain, and may lead to the development of hepatic encephalopathy (nlfindia.com/liverzone/functions.asp).

2.3.9 Bilirubin:

Bilirubin is a yellow pigment. It is formed as a breakdown product of red blood cell hemoglobin. The spleen, which destroys old red cells, releases unconjugated bilirubin into the blood, where it circulates in the blood bound to albumin. The liver takes up bilirubin and "conjugates" it with glucuronic acid to form "water-soluble" bilirubin that can be excreted into bile. Increased production or decreased clearance of bilirubin results in jaundice (nlfindia.com/liverzone/functions.asp).

2.3.10 Hormones:

Liver plays important roles in hormonal modification and inactivation. Chronic liver disease may cause hormonal imbalances. For example, the masculinizing hormone testosterone and the feminizing hormone estrogen are metabolized and inactivated by the liver. Men with cirrhosis, have increased circulating estrogens relative to testosterone derivatives. This may result in testicular atrophy and gynecomastia (nlfindia.com/liverzone/functions.asp).

2.3.11 Drugs:

Most drugs are metabolized by the liver. Especially, oral drugs are absorbed in the intestine and then in the liver, drugs may undergo first-pass metabolism, a process in which they are modified, activated, or inactivated before they enter the systemic

circulation, or they may be left unchanged. In patients with liver disease, drug detoxification and excretion may be dangerously altered, resulting in drug concentrations that are too low or too high or the production of toxic drug metabolites (nlfindia.com/liverzone/functions.asp).

2.3.12 Toxins:

The liver is responsible for detoxifying many chemical agents and poisons including alcohol. Liver disease may inhibit or alter detoxification processes and thus increase the toxic effects of these agents. Additionally, exposure to chemicals or toxins such as alcohol may directly affect the liver, ranging from mild dysfunction to severe and life-threatening damage (nlfindia.com/liverzone/functions.asp).

2.4 Regeneration of the Liver:

The liver has a remarkable capacity to regenerate after injury and to adjust its size to match its host. Within a week after partial hepatectomy, which, in typical experimental settings entails surgical removal of two-thirds of the liver, hepatic mass is back essentially to what it was prior to surgery. Some additional interesting observations include: are too low or too high or the production of toxic drug metabolites (nlfindia.com/liverzone/functions.asp).

In the few cases where baboon livers have been transplanted into people, they quickly grow to the size of a human liver.

When the liver from a large dog is transplanted into a small dog, it loses mass until it reaches the size appropriate for a small dog (nlfindia.com/liverzone/functions.asp).

Hepatocytes or fragments of liver transplanted in extrahepatic locations remain quiescent but begin to proliferate after partial hepatectomy of the host. These types

of observations have prompted considerable research into the mechanisms responsible for hepatic regeneration, because understanding the processes involved will likely assist in treatment of a variety of serious liver diseases and may have important implications for certain types of gene therapy. A majority of this research has been conducted using rats and utilized the model of partial hepatectomy, but a substantial body of confirmatory evidence has accumulated from human subjects (nlfindia.com/liverzone/functions.asp).

2.4.1 The dynamics of liver regeneration:

Partial hepatectomy leads to proliferation of all populations of cells within the liver, including hepatocytes, biliary epithelial cells and endothelial cells. DNA synthesis is initiated in these cells within 10 to 12 hours after surgery and essentially ceases in about 3 days. Cellular proliferation begins in the periportal region (i.e. around the portal triads) and proceeds toward the centers of lobules. Proliferating hepatocytes initially form clumps, and clumps are soon transformed into classical plates. Similarly, proliferating endothelial cells develop into the type of fenestrated cells typical of those seen in sinusoids (nlfindia.com/liverzone/functions.asp).

It appears that hepatocytes have a practically unlimited capacity for proliferation, with full regeneration observed after as many as 12 sequential partial hepatectomies. Clearly the hepatocyte is not a terminally differentiated cell. Changes in gene expression associated with regeneration are observed within minutes of hepatic resection. An array of transcription factors are rapidly induced and probably participate in orchestrating expression of a group of hepatic mitogens. Proliferating hepatocytes appear to at least partially revert to a fetal phenotype and express markers such as alpha-fetoprotein. Despite what appears to be a massive commitment to proliferation, the regenerating hepatocytes continue to

conduct their normal metabolic duties for the host such as support of glucose metabolism (nlfindia.com/liverzone/functions.asp).

2.4.2 Stimuli of hepatic regeneration:

Hepatic regeneration is triggered by the appearance of circulating mitogenic factors. This conclusion was originally supported by experiments demonstrating that quiescent fragments of liver that had been transplanted to extrahepatic sites would begin to proliferate soon after partial hepatectomy, and also that hepatectomy in one of a pair of parabiotic rats led to hepatic proliferation in the other of the pair (nlfindia.com/liverzone/functions.asp).

As might be expected, liver regeneration seems to be supported by a group of mitogens and growth factors acting in concert on several cell types. Some of the major and well-studied players that act together in this process include, hepatocyte growth factor (scatter factor) levels rise to high levels soon after partial hepatectomy. This is the only factor tested that acts by itself as a potent mitogen for isolated hepatocytes cultured in vitro. This factor is also of critical importance in development of the liver, as target deletions of its gene lead to fetal death due to hepatic insufficiency (nlfindia.com/liverzone/functions.asp).

2.5 Pathology:

2.5.1 Cirrhosis:

Is a slowly progressing disease in which healthy liver tissue is replaced with scar tissue, eventually preventing the liver from functioning properly. The scar tissue blocks the flow of blood through the liver and slows the processing of nutrients, hormones, drugs, and naturally produced toxins (en.m.wikipedia.org).

2.5.2 Glycogen storage disease:

The liver cannot control the use of glycogen and glucose because certain enzymes are missing that control the change of sugar (glucose) into its storage form (glycogen) or release of glucose from glycogen (en.m.wikipedia.org).

2.5.3 Fatty liver:

Also known as fatty liver disease (FLD), is a reversible condition wherein large vacuoles of triglyceride fat accumulate in liver cells via the process of steatosis (en.m.wikipedia.org).

2.5.4 Cyst:

Fluid-filled cavities in the **liver** usually cause no signs or symptoms and need no treatment (en.m.wikipedia.org).

2.5.5 Abscess:

Is a pus-filled mass inside the liver, Common causes are abdominal infections such as appendicitis or diverticulitis due to haematogenous spread through the portal vein (en.m.wikipedia.org).

2.5.6 Tumors:

2.5.6.1 Benign:

If you are told your tumor is “benign,” that means it is not cancerous. It is similar to cancer because the growth is a result of abnormal cells. However, unlike cancer, it is unable to spread to other areas of the body (such as the brain or lungs) and it does not affect nearby tissue. It is a contained mass that stays where it grows (**Cooper 1992**).

On its own, a benign tumor is not dangerous. However, the location of the tumor is what poses the threat. If the mass puts pressure on a primary nerve, a main artery, or compresses brain matter, even a benign tumor can cause serious problems. Some suspected causes of benign tumors include a traumatic injury at the tumor location, chronic inflammation (or long-term stress that leads to inflammation), an undetected infection, or diet (**Cooper 1992**).

Most common benign tumors are , adenomas (epithelial tissue that covers the organs and glands), meningiomas (brain and spinal cord), fibromas or fibroids (connective tissue of any organ – most commonly found in the uterus), papillomas (skin, breast, cervix, and mucus membranes), lipomas (fat cells), nevi (moles), myomas (muscle tissue), hemangiomas (blood vessels and skin), neuromas (nerves), osteochondromas (bones) (**Cooper 1992**).

Depending on the location and size of a benign tumor, treatment might not be necessary. Doctors will monitor it, track patient symptoms and do tests at specific intervals (**Cooper 1992**).

Benign tumors are often surrounded by a protective “sac” a mechanism performed by your immune system – that segregates it from the rest of your body and enables it to be easily removed (**Cooper 1992**).

If you are diagnosed with a benign tumor, altering your diet to an anti-cancer regimen is sound advice. Some benign tumors can become malignant but it’s rare. Even when they are removed, your doctor will schedule regular tests periodically to ensure no additional tumors form (also a rare occurrence).

Overall, benign tumors respond well to treatment and the prognosis is usually favorable (**Cooper 1992**).

2.5.6.2 Malignant:

If your doctor determines that you have a malignant tumor, that means the mass is cancerous. The word malignant is Latin for “badly born.” This type of tumor has the ability to multiply uncontrollably, to metastasize (spread) to various parts of the body and invade surrounding tissue (**Cooper 1992**).

Malignant tumors are formed from abnormal cells that are highly unstable and travel via the blood stream, circulatory system and lymphatic system. Malignant cells do not have chemical adhesion molecules to anchor them to the original growth site that benign tumors possess (**Cooper 1992**).

There are many suspected causes of cancer – some are widely accepted by the medical community while others are not. Obesity, smoking, alcohol consumption, poor diet, environmental pollution, heavy metal exposure and household toxins are a few culprits that may lead to cancer in your body (**Cooper 1992**).

Most Common malignant tumors are, Sarcomas (connective tissues such as muscle, tendon, fat, and cartilage) and carcinomas (organs and gland tissue such as the breast, cervix, prostate, lung, and thyroid) (**Cooper 1992**).

Malignant tumors may not have symptoms initially and the first indication that something isn’t right may be the detection of a painless lump. These types of tumors are “elastic,” which enables them to grow fairly large before they are detected (**Cooper 1992**).

As they grow and begin to press against organs, blood vessels and nerves, pain and general soreness at the site may occur (**Cooper 1992**).

2.5.7 Metastases:

Occurs when cancer spreads from its original location (primary tumor) to a new part of the body (en.m.wikipedia.org).

2.6 Computed tomography:

2.6.1 Introduction:

Computed tomography (CT) is an imaging procedure that uses special x-ray equipment to create detailed pictures, or scans, of areas inside the body. It is also called computerized tomography and computerized axial tomography (CAT) (**Serum 2000**).

The term tomography comes from the Greek words tomo (a cut, a slice, or a section) and graphy (to write or record). Each picture created during a CT procedure shows the organs, bones, and other tissues in a thin “slice” of the body. The entire series of pictures produced in CT is like a loaf of sliced bread you can look at each slice individually (2-dimensional pictures), or you can look at the whole loaf (a 3-dimensional picture). Computer programs are used to create both types of pictures (**Serum 2000**).

Most modern CT machines take continuous pictures in a helical (or spiral) fashion rather than taking a series of pictures of individual slices of the body, as the original CT machines did. Helical has several advantages over older CT techniques: it is faster, produces better 3-D pictures of areas inside the body, and may detect small abnormalities better. The newest CT scanners, called multislice CT or multidetector CT scanners, allow more slices to be imaged in a shorter period of time (**Serum 2000**).

In addition to its use in cancer, CT is widely used to help diagnose circulatory (blood) system diseases and conditions, such as coronary artery disease (atherosclerosis), blood vessel aneurysms, and blood clots; spinal conditions; kidney and bladder stones; abscesses; inflammatory diseases, such as ulcerative colitis and sinusitis; and injuries to the head, skeletal system, and internal organs. CT can be a life-saving tool for diagnosing illness and injury in both children and adults (**Serum 2000**).

2.6.2 Basic principles:

CT slices are oriented vertical to the body's axis. They are usually called axial or transverse sections. For each section the x-ray tube rotates around the patient to obtain a preselected section thickness (**Serum 2000**).

Most CT systems employ the continuous rotation and fan beam design: with this design, the x-ray tube and detector are rigidly coupled and rotate continuously around the scan field while x-rays are emitted and detected (**Serum 2000**).

Thus, the x-rays, which have passed through the patient, reach the detectors on the opposite side of the tube (**Serum 2000**).

The fan beam opening ranges from 40° to 60° , depending on the particular system design, and is defined by the angle originating at the focus of the x-ray tube and extending to the outer limits of the detector array (**Serum 2000**).

Typically, images are produced for each 360° rotations, permitting a high number of measurement data to be acquired and sufficient dose to be applied. While the scan is being performed, attenuation profiles, also referred to as samples or projections, are obtained (**Serum 2000**).

Attenuation profiles are really nothing other than a collection of the signals obtained from all the detector channels at a given angular position of the tube-detector unit. Modern CT systems acquire approximately 1400 projections over 360° , or about four projections per degree. Each attenuation profile comprises the data obtained from about 1500 detector channels, about 30 channels per degree in case of a 50° fan beam. While the patient table is moving continuously through the gantry, a digital radiograph (scanogramm or localizer) is produced on which the desired sections can be planned (**Serum 2000**).

For a CT examination of the spine or the head, the gantry is angled to the optimal orientation (**Serum 2000**).

2.6.3 Data acquisition:

2.6.3.1 Data acquisition modes:

As it was mentioned earlier during the data acquisition the x-ray source and the detector are rotating around the axis of rotation of the gantry and acquiring projection data from the object located between them. The rotational motion can be continuous or stepping. In continuous mode the projection data is blurred and it is relative to the arc rotated during the readout time of the detector. In case of fast readout detectors this is negligible, and this effect can be controlled by the adjustment of the rotation speed to the readout time. If the rotational motion is done in steps (step and shoot mode) the blurring can be avoided, but the start and stop cycles of the motion increase the acquisition time. Nevertheless, this latter method is useful to image ex-vivo samples with high resolution, while the continuous motion is beneficial to image living and moving objects (**Serum 2000**).

2.6.3.2 Circular scan:

If the holder of the object stands still during the rotation, then the x-rays draw a circular orbit on the surface of the object. This acquisition mode called circular scan. In this case the x-rays in the middle of the field of view are parallel to the reconstruction plane, therefore the image quality of the corresponding slices are excellent. However, the slices located at the edge of the field of view has an increasing angle to the x-rays, therefore their image quality is deteriorated and characteristic artefacts appear (cone-beam artefact). In circular mode the acquisition time is equal to the duration of one rotation and the axial scan range is to one axial field of view (**Serum 2000**).

2.6.3.3 Spiral scan:

In order to image an object extending over the axial field of view of the detector multiple circular scan can be performed one after the other. This can be time consuming and the image quality will vary along the z-axis due to the cone-beam artefact mentioned earlier. Another option is to continuously move the table during the rotation. The x-rays draw a spiral on the surface of the object, therefore this acquisition mode is called to helical or spiral scan (**oftankonyv.reak.bme.hu**).

Similarly, to the third generational human CT systems the ratio of the table translation over one rotation to the axial field of view is called to *pitch*. It is equal to one, when the table moves exactly one axial field of view per rotation. If the pitch was bigger than one there are gaps in the axial coverage and interpolation should be used to calculate the missing raw data. In contrary if the pitch was bigger than one the spiral orbits will overlap, so the same region is scanned over more than one rotation. The higher the pitch the lower the acquisition time, however the image quality is also lower (**oftankonyv.reak.bme.hu**).

The biggest advantage of the spiral scan is that reconstructed slices have homogeneous image quality and the acquisition time is shorter in compare to multiple circular scanning. Although the scan range has to be extended in order to reconstruct the entire selected volume, this usually does not cause problems in practice (oftankonyv.reak.bme.hu).

Table (2.1) Comparison of the parameters of different scan modes AFOV – axial field of view, p – pitch.

	Circular	Multi circulars	Helical/Spiral
Number of rotations (N)	1	N	SR/p
Rotation time (t_{rot})	t_{rot}	t_{rot}	t_{rot}
Table travel speed	0	0	$(AFOV \cdot p) / t_{rot}$
Scan range (SR)	AFOV	$N \cdot AFOV$	SR
Scan time	t_{rot}	$N \cdot t_{rot}$	$t_{rot} \cdot SR / p$

2.6.3.4 Other orbits:

Reconstructions based on filtered back projection (FBP) algorithm gives the best result if the data was collected with homogeneous sampling. This requires collecting the projection data with equal sampling both along the table translation and over the gantry rotation. Conversely, iterative algorithms can reconstruct

images from incomplete projection data or from smaller number of projections making possible to reconstruct the volume even in special cases, when it was not possible to perform a complete, uniform scanning of the object. Iterative algorithms are used for example for scanning large sized printed circuit boards, where depth information is ensured by scanning along a surface with largest available solid angle (oftankonyv.reak.bme.hu).

2.6.3.5 Acquisition parameters:

The parameters are usually selectable on a cone-beam CT system console together with their description and their typical values are shown in the (oftankonyv.reak.bme.hu).

Table (2.2) Parameters are usually selectable on a cone-beam CT system console

Parameter	Description	Typical range
Tube voltage	The accelerator voltage of the x-ray tube. Determines the maximum energy of the x-ray beam.	Discrete values 30 - 80 kVp
Tube current	The heating current of the x-ray cathode. Defines the amount of the accelerated electrons, thus the intensity of the generated x-ray beam.	Continuous values 0.1 – 10 mA
Exposure time	Integration time of the x-ray detector	10 – 5 000 ms
Number of projections	Number of projections collected per rotation. It is also referred as angular sampling.	180 – 720

Binning	Possibility to sum the data of the neighboring pixels of the detector. It lowers the noise of the raw data but also decrease the achievable spatial resolution.	1x1 – 4x4
Pitch	The ratio of the table translation over one rotation to the axial field of view. It defines the sampling in the z-direction.	0.5 – 1.5
Zoom factor	Defined as a ratio of the field of view to the active surface of the detector.	~1.2x – 1000x

2.6.3.6 Raw data processing:

The Figure 3 shows a practical example of the raw data processing performed after the data acquisition. The data is acquired by a frame grabber card connected directly to the X-ray detector and transferred to the memory of the acquisition PC. In order to speed up the read out of the detector several pixels are read out in parallel and their signal is serialized. Therefore, the first step is to sort them into the right order to form the columns and rows. This step is called to DE interlace. If the full resolution is not required, then the projections can be resized (**oftankonyv.reak.bme.hu**).

The data is transferred form the system memory to the memory of the GPU (graphical processing unit), which can perform the reconstruction in real time together with all the projection level corrections. Following the offset, gain and bad pixel corrections the projections are saved for further processing and also transferred to the reconstruction where following a geometrical correction step they are back projected. After all the data is processed the reconstructed volume is displayed and saved (**oftankonyv.reak.bme.hu**).

2.6.4 Corrections:

2.6.4.1 Offset correction:

The dark current (also known as offsets) is a leaking current on the photodiodes, which cause a measurable signal for a detector without X-ray illumination. The magnitude of the signal increases linearly with exposure time, and in case of $t_{\text{exp}}=0$, its value is greater than zero. Each offset value of the detector pixel changes due to temperature, increasing the temperature with 10 Celsius degrees causes doubled value. Thus, if the detector environment temperature changed, it is necessary to recalibrate the offset. The dark current value varying from pixel to pixel, its detector surface distribution is not uniform (oftankonyv.reak.bme.hu).

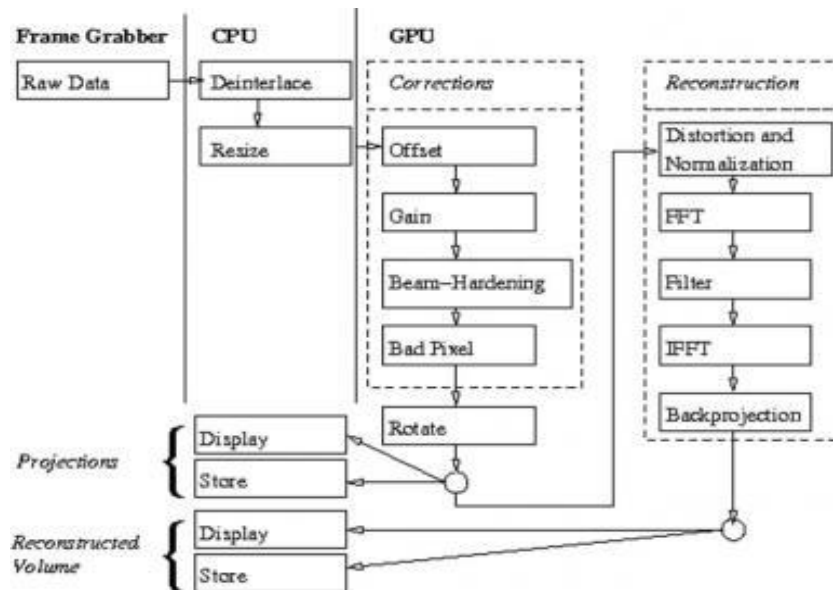


Figure (2.5) Raw data processing and reconstruction steps in a cone-beam CT system (oftankonyv.reak.bme.hu).

During the calibration of the dark current, each pixel is measured on the further applied exposure time, and the resulting matrices are stored and subtracted from collected raw images. If the offset matrices are misscalibrated, slightly dark circles appear on the homogeneous areas of the reconstructed image (oftankonyv.reak.bme.hu).



Figure (2.6) Offset image of a 7-panel detector (RadEye7H). It can be seen that each panel has different dark current average from one another; the highest (light) is from the left of the first and 4 panel, while the lowest (dark) is in the sixth panel (oftankonyv.reak.bme.hu).

2.6.4.2 Gain correction:

For good image quality, it is needed that for homogeneous radiation in the detector should result homogeneous images. The individual diodes have different response for the input signal for each pixel, because of the nonlinear sensitivity (oftankonyv.reak.bme.hu).

The target of gain calibration is to change each pixel's locally varying characteristics to a common linear response function of the detector. During the calibration the response functions for each pixel is determined according to a predefined tube current and tube voltage. In general, the input signal is the multiplication of the tube current and exposure time, but in this case the

time-dependency is examined in addition to constant current. The characteristic of the signal-response function can be described accurately with polynomial; its order depends on the specific system (e.g. the type of detector). After the correction, the attenuated X-rays should result same intensity in each pixel, if a homogeneous and constant thickness of absorbing object is placed between the x-ray source and detector (oftankonyv.reak.bme.hu).

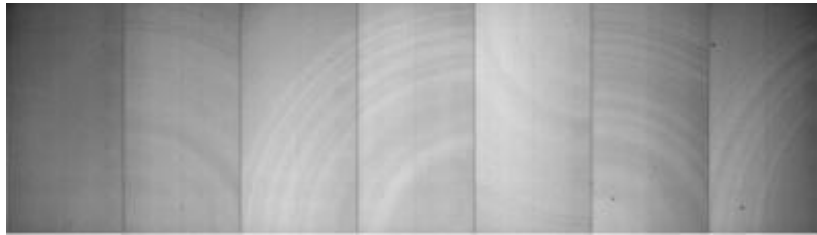


Figure (2.7) Image of a 7-panel detector (RadEye7H) without gain correction. One can see that in spite of the homogeneous illumination the detector image is not homogeneous because of the different sensitivity of individual pixels (oftankonyv.reak.bme.hu).

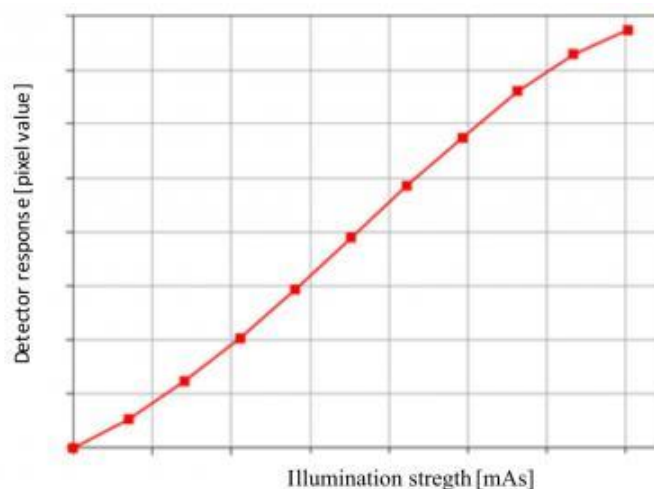


Figure (2.8) The X-ray detector response function in term of the illumination. If the gain correction values are obsolete, then ring artefacts appear on the homogeneous areas of reconstructed images, like the failure of dark current correction (oftankonyv.reak.bme.hu).

2.6.4.3 Beam-hardening correction:

For monochromatic beam the attenuation in a homogenous object is described by the Lambert-Beer law. In voxelized environment this can be written as follows:

$$y_i = I_0 \cdot e^{-\sum_{j=1}^N (l_{ij} \mu_j)}$$

Where

y_i is the intensity measured in the i -th pixel

I_0 intensity comes from source

μ_j the mass attenuation coefficient in the j -th voxel

l_{ij} the length of the beam passing through the j -th voxel comes from the source to the i -th pixel

The Feld Kamp-type reconstruction is based on monochromatic beam. In practice, the spectrum of X-ray is an extended continuous function. Because the absorption of materials are energy dependent, characteristic artefacts arise on the uncorrected reconstructed image that a real uniform attenuation area (e.g. water-filled cylinder) has a descending intensity profile towards the center. Since for the lower energies have greater attenuation, in a certain thickness of medium the low-frequency components can disappear from the spectrum. The name refers to this phenomenon, the spectrum of high-energy "hard" part retained after the transmission. Accordingly, on the reconstructed images of a homogeneous phantom the absorption is not uniform but decreases toward the center of the phantom. This phenomenon is well explained by the fact that at the edge of the phantom during penetration, even a low-energy components are also present, where the absorption is higher, but they are completely absorbed in the middle (oftankonyv.reak.bme.hu).

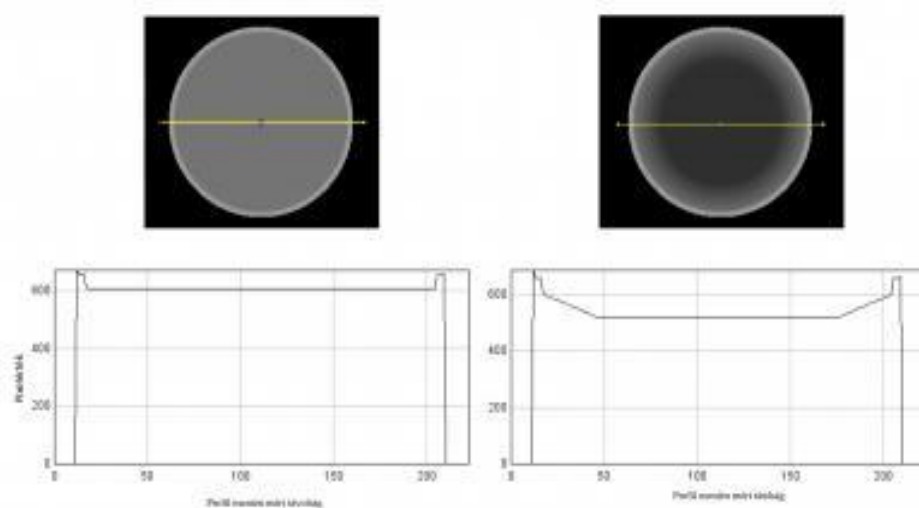


Figure (2.9) Beam-hardening effect and correction. The upper left picture shows a water-filled cylinder beam-hardening corrected homogeneous cross-sectional image, below the yellow line corresponding profile curve. (oftankonyv.reak.bme.hu).

Correction can be made by hardware or software filtering. In case of hardware filtering (see Mechanical filters in Section) metal filter (e.g. aluminum) mounted in front of the X-ray tube absorb the low-energy parts of the spectrum directly after the exit from the tube. Unfortunately, the filters are only partially selective and beside the low-energy components, the high-energy range of the spectrum are reduced, thereby reduce the light intensity and increase the image noise. Therefore, in practice, in addition to the hardware filter, software algorithms are applied on the projections or reconstructed images (oftankonyv.reak.bme.hu).

2.6.4.4 Bad pixel correction:

A pixel is assigned as defective if, after the above corrections (offset, gain, and projection level beam-hardening) the input signal of this pixel is significantly different from its environment. If a pixel's dark current is too large, the response during exposure can be saturated and therefore false information can be gained out

of it. The aim of the calibration is to find these pixels and to correlate with the saturation value. Another problem if the intensity of a pixel in the offset-corrected image is very different from the average, the gain correction cannot be used because the pixel value is too low (does not respond to illumination) or saturates over a particular exposure time. The defective pixels found in the calibration can be stored in a mask, and using the neighboring pixels based interpolation can be corrected. The defective pixels cause usually a sharply contrasting environment, circular artefacts in the reconstructed image (**oftankonyv.reak.bme.hu**).

2.6.4.5 Geometric calibration:

Although during the CT acquisition, the X-ray detector and tube mounted on a common mechanical frame and performs rotation through pre-known positions; but for reconstruction of the images with high spatial resolution ($\sim 10\mu\text{m}$) the relation of the tube and the detector to the axis of rotation should be determined greater precision than the mechanical accuracy. (**oftankonyv.reak.bme.hu**).

The determination of the geometric parameters of the cone-beam CT coordinate system described on Coordinate system of the cone-beam CT) can be done in many ways. In the course of the most commonly used calibration procedure a phantom with high attenuation point objects (e.g. ball bearings) with known distance from each other is measured. When the center of objects found in each projection of the total turn around, a continuous, angular position dependent model can be fit each center of masses. The system geometry can be calculated from the fitting parameters. The parameters can be constants or gantry angle (**oftankonyv.reak.bme.hu**).

A proper model function, which is based on the following equations:

$$Y(\theta) = D \frac{-x_{\nu} \sin(\theta) + y_{\nu} \cos(\theta)}{D - d + x_{\nu} \cos(\theta) + y_{\nu} \sin(\theta)} + E_y(\theta)$$

$$Z(\theta) = D \frac{-z_{\nu}}{D - d + x_{\nu} \cos(\theta) + y_{\nu} \sin(\theta)} + E_z(\theta)$$

Where

D distance between focal point and the detector

d distance between focal point and axis of radius of rotation

E_y and E_z is the distance between the focal point and the normal of the detector placed to the center of the detector

$x_{\nu}, y_{\nu}, z_{\nu}$ position of the point sources

Y, Z the mapped coordinates of the point sources in the coordinate system of the detector

θ gantry position

2.6.5 Image display:

After the CT image has been reconstructed, it exits the computer in digital form. This must be converted to a form that is suitable for viewing and meaningful to the observer. In CT the digital reconstructed image is converted into a gray scale image for interpretation by the radiologist. Because a diagnosis is made from this image, it is important to present this image in a way that facilitates diagnosis. The target of gain calibration is to change each pixel's locally varying characteristics to a common linear response function of the detector. During the calibration the response functions for each pixel is determined according to a predefined tube

current and tube voltage. In general, the input signal is the multiplication of the tube current and exposure time, but in this case the time-dependency is examined in addition to constant current. The characteristic of the signal-response function can be described accurately with polynomial; its order depends on the specific system (e.g. the type of detector). After the correction, the attenuated X-rays should result same intensity in each pixel, if a homogeneous and constant thickness of absorbing object is placed between the x-ray source and detector (oftankonyv.reak.bme.hu).

2.6.5.1 Ct number:

The Hounsfield unit (HU) scale is a linear transformation of the original linear attenuation coefficient measurement into one in which the radiodensity of distilled water at standard pressure and temperature (STP) is defined as zero Hounsfield units (HU), while the radiodensity of air at STP is defined as -1000 HU. In a voxel with average linear attenuation coefficient μ , the corresponding HU value is therefore given by:

$$HU = 1000 \times \frac{\mu - \mu_{water}}{\mu_{water} - \mu_{air}}$$

Where μ_{water} and μ_{air} are respectively the linear attenuation coefficients of water and air (Feeman, Timothy G. 2010).

Thus, a change of one Hounsfield unit (HU) represents a change of 0.1% of the attenuation coefficient of water since the attenuation coefficient of air is nearly zero (Feeman, Timothy G. 2010).

It is the definition for CT scanners that are calibrated with reference to water (Feeman, Timothy G. 2010).

2.6.6 Instrumentation:

A scanning gantry that includes the collimated x-ray source, the detectors, the computer for data acquisition, the image reconstruction system, motorized patient-handling table, the CT viewing console.

The major technical difference between various commercial scanners lies in the gantry design and the number and the type of x-ray detectors used (**Feeman, Timothy G. 2010**).

2.6.7 Advantage & disadvantage:

2.6.7.1 Advantage:

Quick and painless, can help diagnose and guide treatment for a wider range of conditions than plain X-ray, detect or exclude the presence of more serious problems and used to check if a previously treated disease has (**Frush DP 2004**).

2.6.7.2 Disadvantages:

Small increased risk of cancer in future from exposure to ionizing radiation (X-rays). Risk is greater for children, uses higher doses of radiation than plain X-ray, so the risks (while still small) are generally greater than for other imaging types. Injection of a contrast medium (dye) can cause kidney problems or result in allergic or injection-site reactions in some people. Some procedures require anesthesia (**Frush DP 2004**).

Table (2.3): Show different HU for different densities:

Substance	HU
Air	−1000
Lung	−500
Fat	−100 to −50
Water	0
<u>CSF</u>	15
Kidney	30
Blood	+30 to +45
Soft Tissue, Contrast	+100 to +300
Bone	+700 (cancellous bone) to +3000 (cortical bone)

2.6.8 Previous studies:

-Mohamed Alhaj Albasher, 2013 (Role of tri-phasic spiral CT in the evaluation of liver tumors)

He found that using of the triple phase spiral CT make clearly demonstrate and highlight many hepatic lesions (vascular & non-vascular).

It is important to high injection rates and appropriate bolus timing.

Spiral CT scan should be delayed 30-50 sec after injection of contrast agent for greater enhancement of the liver.

In forthcoming studies should increase sample size and correlate focal liver lesions with age, habits and patient condition.

Further studies should compare the amount of contrast and rate of injection with the degree of enhancement of the lesions.

-Al-Mutasim, 2006 (Role of US vs CT in diagnoses hepatic focal lesions)

He found that, the most common type of focal liver lesions is HCC and showed in arterial phase inhomogeneous enhancing masses with focal area of necrosis, and recommend that it is important to use high injection rates and appropriate bolus timing.

Spiral CT scan should be delayed 30-50 sec after injection of contrast agent for greater enhancement of liver.

In forthcoming studies should increase sample size and correlate foal liver lesion with age, habits and patient condition.

Future studies should compare the amount of contrast and rate of injection with the degree of enhancement of the lesion.

-Hafeez, S. et.al (2011). Triphasic computed tomography (CT) scan in focal tumor liver lesions.

Triphasic CT scan is a good non-invasive tool and can be used as first line imaging modality for differentiating benign and malignant focal liver lesions.

Benign lesions like hemangioma can be reliably differentiated from malignant liver lesion; therefore, unnecessary biopsies can be avoided. It is also particularly useful for hyper vascular lesions which can be easily missed on routine CT scanning.

In 94 patients, 375 liver lesions were detected. The nature of the lesion was confirmed in 326 lesions

(87%). Six of 11 enhancement patterns were always due to benign disease and caused by areas with hyper- or hypo perfusion, hemangiomas, cysts, focal nodular hyperplasia, or benign but non-specified lesions.

Two of 11 patterns were always due to malignant disease, and one pattern was due to malignant disease in 38

(97%) of 39 patients with known malignancy elsewhere or with chronic liver disease. The other two patterns were seen in metastases and partly fibrosed hemangiomas.

Materials & Methods

3.1 CT system:

CT machine used for collecting data are Toshiba CT scanner (64 slice) and Neo Soft (16 slice) with 120 kV and 200 mA.

3.2 Population:

The data has been collected from Royal Scan International Hospital & Police Hospital, the study included Sudanese patient, there ages between 36 - 86 y and all patients done triphasic CT scan.

3.3 Sample size:

50 patients (21 females and 29 males).

3.4 Patient preparation:

Asses the clinical problems & medical history, includes the indication of the study, contrast allergies, renal impairment etc.

3.5 Equipments:

CT scanner and automatic injector. CT scanner



Figure (3.1) Automatic injector



Figure (3.2) CT Scanner and control console

3.6 Contrast media:

3.6.1 IV HOCM or LOCM:

3.6.1.1 Total amount of contrast:

Weight < 75kg = 100cc

Weight 75-90kg = 120cc

Weight > 90k = 150cc

3.6.1.2 Injection rate:

5cc/sec through an 18-gauge and 3-4cc/sec through a 20 gauge

3.6.2 Oral

3.7 Technique:

Scan area from the lower border of diaphragm to symphysis pubic, patient lies supine, feet first, rise hands above head, scans are performed during normal inspiration, gantry angle zero, 10 mm slice thickness are selected through the entire abdomen.

3.8 Phases:

3.8.1 Arterial: After 35 secs from contrast injection.

3.8.2 Portovenous: After 50 secs contrast injection.

3.8.3 Venous: After 75 secs contrast injection.

3.8.3 Delay: After 5 min contrast injection.



Figure (3.3) Gastrographin (CM)

Results

Table (4.1) Distribution of population by gender:

Gender	Frequency	Percentage
Male	24	48
Female	26	52
Total	50	100%

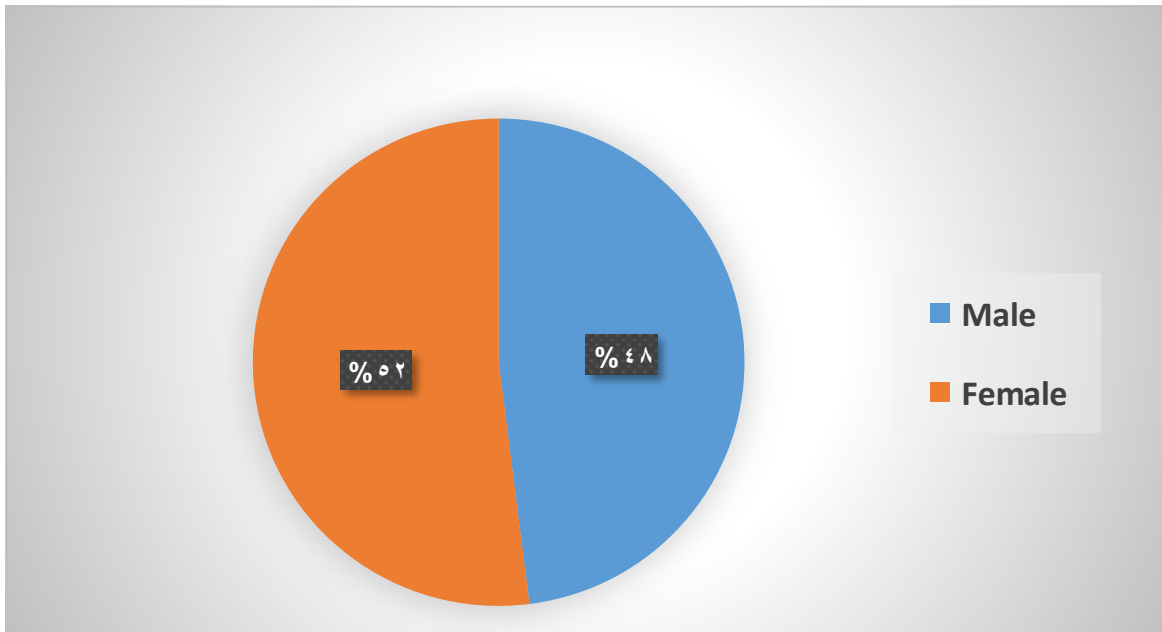


Figure (4.1) Distribution of population by gender

Table (4.2) Type of liver tumors by gender:

Gender	Benign	Malignant	Total
Male	10	14	24
Female	4	22	26
Total	14	36	50

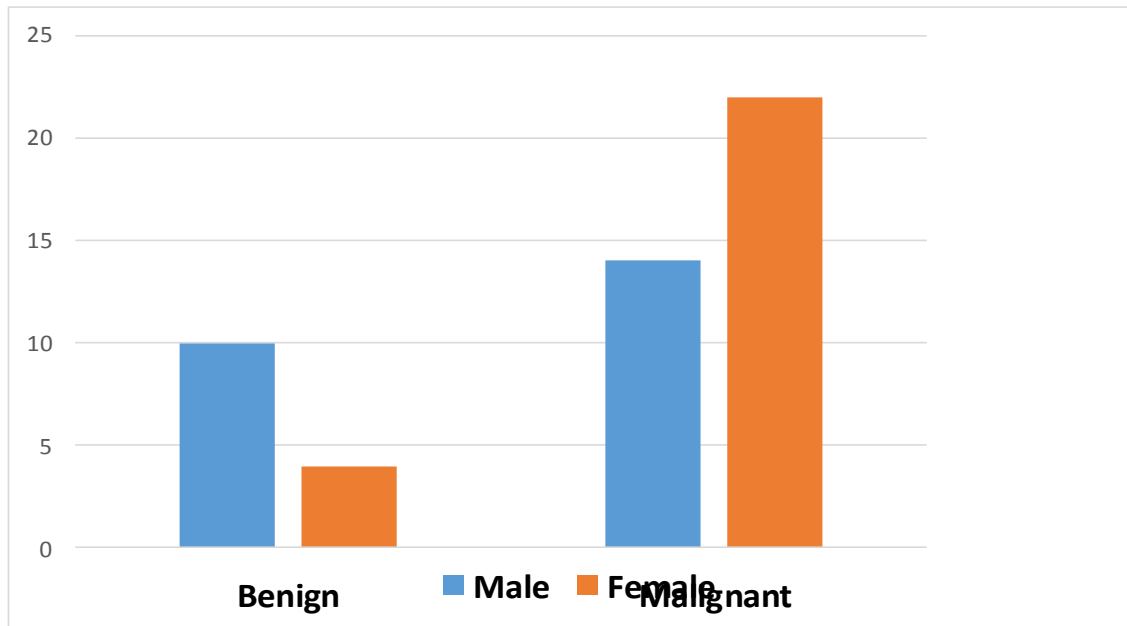


Figure (4.2) Type of liver tumors by gender

Table (4.3) Type of liver tumors by age:

Age	Malignant	Benign	Frequency
36-44	3	3	6 (12%)
45-53	6	2	9 (18%)
54-62	11	5	16 (32%)
63-71	7	1	8 (16%)
72-80	5	2	7 (14%)
81-89	4	1	4 (8%)
Total	36 (72%)	14 (28%)	50 (100%)

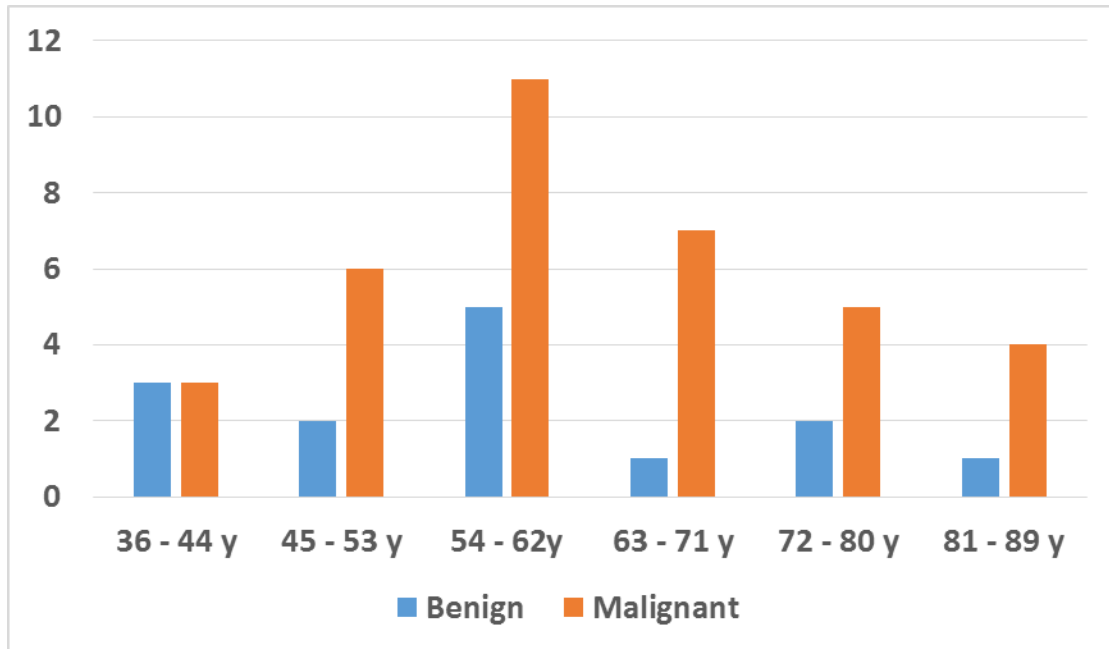


Figure (4.3) Type of liver tumors by age

Table (4.4) show degree of enhancement of tumor related to liver parenchyma:

Lesion	Benign	Malignant
Arterial	Hyper dense	Hyperdense
Portovenous phase	Isodense	Isodense
venousphase	Hyperdense	Hypodense

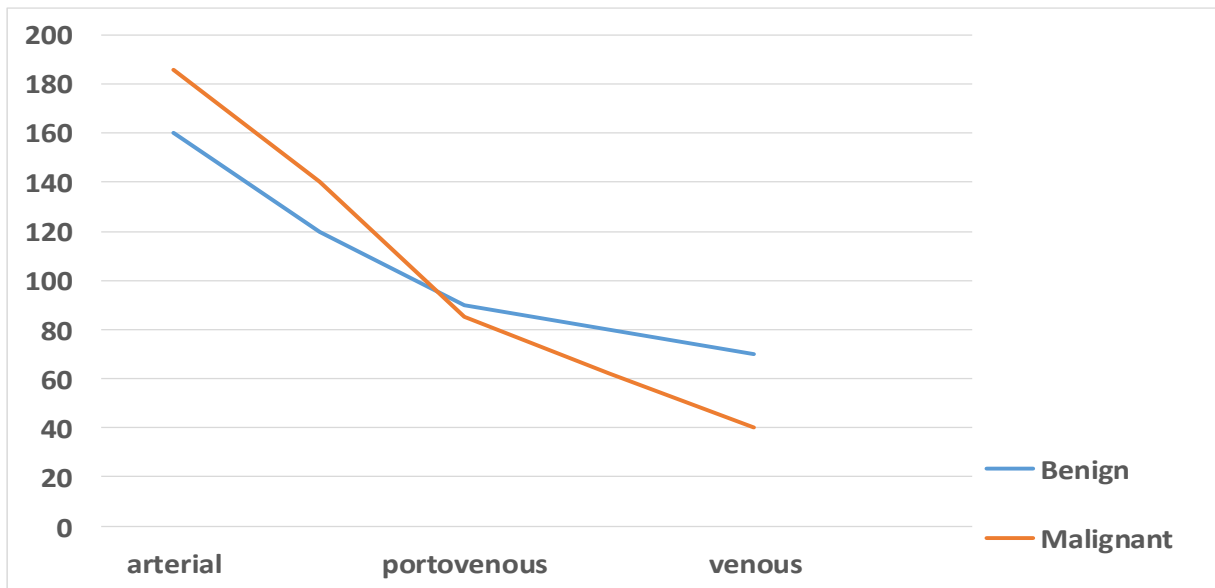


Figure (4.4) Diagram shows correlation between degree of enhancement of benign and malignant tumor with time

5. 1 Discussion:

A total of 50 patients were selected randomly, 24 are males (48%) while the rest 26 are females (52%).

Table (4.1) and Figure (4.1) shows distribution of population by gender 24 males (48%) and 26 (52%) females. Table (4.2) and Figure (4.2) shows that the females are most common effected by malignant tumors than males. Table (4.3) and Figure (4.3) represent the type of liver tumors by age, and shows that the age between 54 and 62 is the most common age for the liver to affect by malignant tumors. Table (4.4) Represent the degree of enhancement of liver tumors related to liver parenchyma and shows that the malignant tumors appear as hyper dense area comparing to the normal liver parenchyma at arterial phase, because of rapid administration of contrast media inside it & that because it is one of the hyper vascular lesion (rapid wash-in and rapid wash-out), the enhancement appears heterogeneous in shape, 8 of the patient have secondary malignant tumor (Metastasis) at different organs (kidney-bladder-gall bladder and pancreas).

Benign tumors appear as hypodense area compare to liver parenchyma at arterial phase due to of low administration of contrast media to the tumor, and hyper dense area at portovenous phase, the enhancement appears homogenous in shape, it had no metastasis because it's a benign tumor.

Figure (4.4) Diaphragm shows correlation between degree of enhancement of benign and malignant tumor with time.

5.2 Conclusion:

Tri-phasic spiral computed tomography is the golden standard examination used to evaluate the liver tumors (Malignant-Benign), that's because it gives us the pathology at different phases (arterial – portovenous – venous-delay), appearance of enhancement by time (homogenous, heterogeneous) and the vascularity of the tumor (speed of wash in & wash out).

Reconstruction of images should be at 2mm interval.

By following the scan protocols and use contrast media by its true dose, a good diagnostic image can be provided.

5.3 Recommendation:

Tri-phasic spiral CT must be used with as standard protocol for evaluation the liver tumors, because it gives us a clearly image of normal liver parenchyma and any pathology that effect it, so that let the radiologists to write full report.

Contrast media should be given by its significant doses.

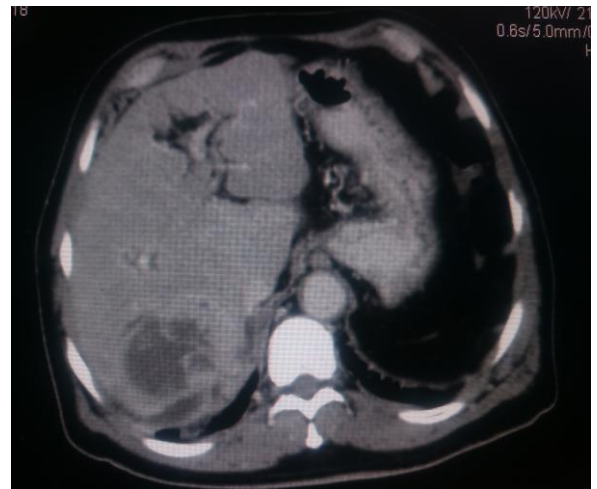
Scan delay should be 35 sec after injection for more enhancement.

For better result the ministry of health must provider better and more updated CT scans (at least 64 slice)

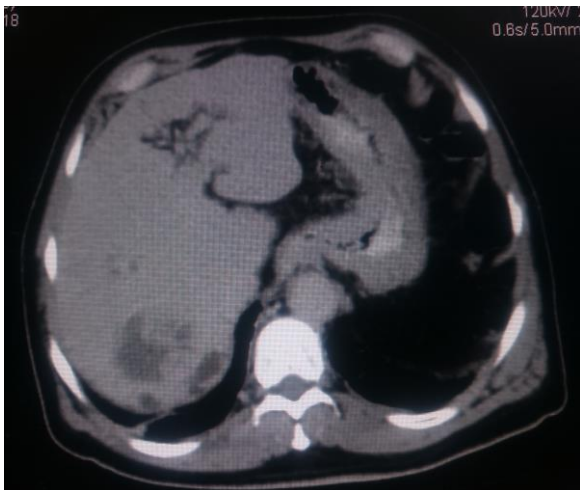
Appendices (A)



(A)



(B)



(C)

Fig. (A.1) Axial Tri-phasic spiral CT images for male, 52y showed large liver mass (HCC) with central necrosis.

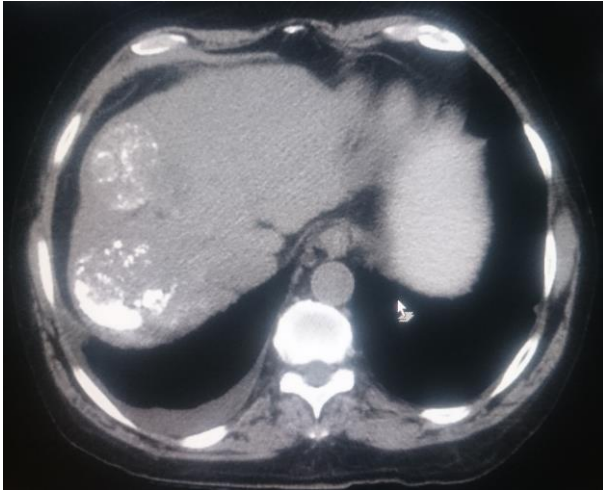
(A)Arterial phase rapid wash-in contrast into tumor.

(B)Porto-venous phase.

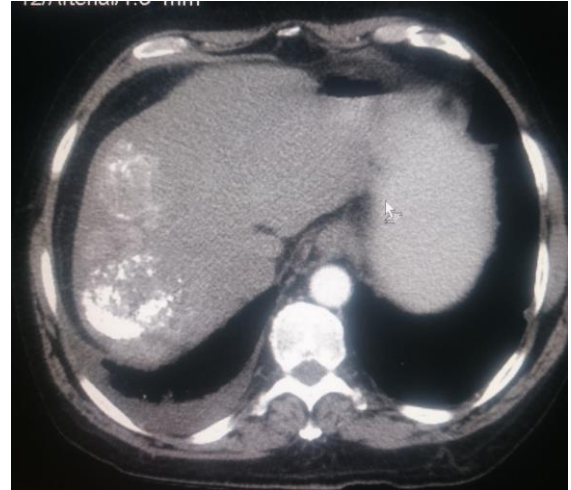
(C)Delay.



Fig. (A.2) Coronal Tri-phasic spiral CT images for male, 52y showed large liver mass (HCC) with central necrosis.



(A)



(B)

Figure (A.3): Axial Tri-phasic CT images with (A) and without (B) contrast showed two calcified tumors.

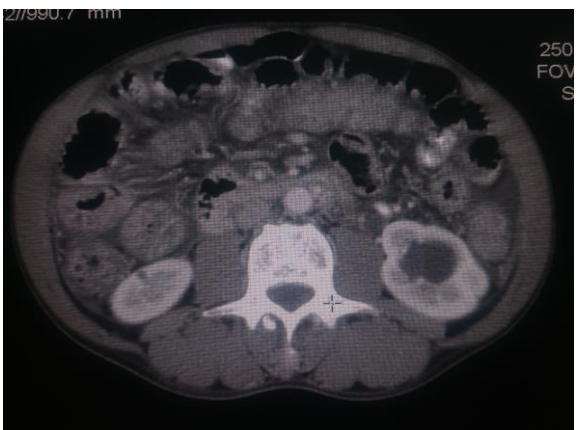
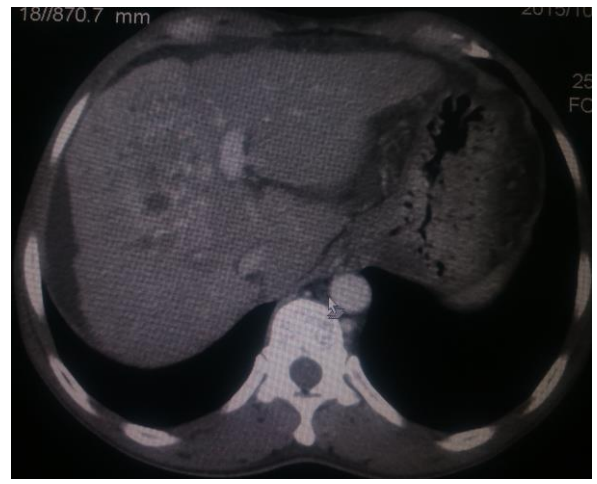
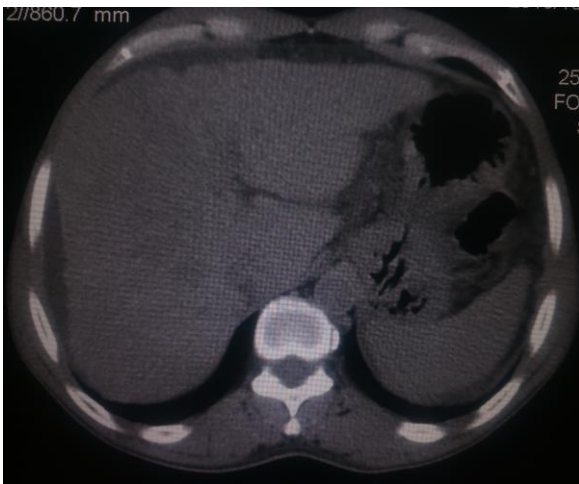


Figure (A.4): Axial tri-phasic spiral CT images shown HCC with metastases in left kidney.

(A) Axial abdomen without contrast.

(B) Axial arterial phase.

(C) Lt kidney cyst.

Appendices (B)

Evaluation of liver tumors by using triphasic spiral CT

Data collection sheet

1-Sex: Male ☐ Female ☐

2-Age:

3-Amount of contrast: ml

4-Type of tumor: Benign ☐ Malignant ☐

5-If malignant, did it have metastases: Yes ☐ No ☐

6-If Yes, in which organ:.....

7-Type of enhancement:.....

8-Ct number at arterial phase:

Tumor Normal tissue Aorta IVC

9-Ct number at portal phase:

Tumor Normal tissue Aorta IVC

10-Ct number at delay:

Tumor Normal tissue Aorta IVC

References

- Biofortified. (2012)glowing-phagocytosis.
- Bishop, M., Fody, E., & Schoeff, I. (2010). Clinical Chemistry: Techniques, principles, Correlations.
- Carlson SK, Johnson CD, Bender CE, Welch TJ (2000) CT of focal nodular hyperplasia of the liver.
- Differentiation between true focal liver lesions and psudolesions in patients with fatty liver: evaluation of helical CT criteria.
- Foley WD, Mallisee TA, Hohenwarter MD, Wilson CR, Quiroz FA, Taylor AJ. (2000) Multiphase hepatic computed tomography with a multirow detector computed tomography scanner.
- Hafeez, S., Alam, M., Sajjad, Z., Khan, Z., Akhter, W., Mubarak, F. (2011). Triphasic computed tomography (CT) scan in focal tumoral liver lesions.
- Hiatt JR, Gabbay J, Buscutti RW(1994), Surgical anatomy of the hepatic arteries in 1000 cases.
- Johnson PT, Fishman EK. IV Contrast selection for MDCT (2006) Current thoughts and practice.
- Journal of Rawalpindi Medical College (2011) Ct scan appearances of different focal liver lesions.
- Snell S. 2008. Clinical anatomy by regions 8^{Ed}.
- Liau KH, Blumgart LH ,DeMatteo RP(2004) Segment-oriented approach to liver resection.
- Moeller T.B,Reif E.(2007). Pocket atlas of sectional anatomy 3rd edition.

- Szklaruk J, Silverman PM, Chamsangavej C. (2003) Imaging in the diagnosis, staging, treatment and surveillance of hepatocellular carcinoma.
- Sunheimer, R., & Graves, L. (2010). Clinical Laboratory Chemistry. Upper Saddle River: Pearson.
- Thomas M. Simon A. Jackson RM. (2005) Cross-sectional Imaging Made Easy.
- Wagner T. 1999. Handbook of computer vision.
- www.en.m.wikipedia.org
- www.oftankonyv.reak.bme.hu